Contents lists available at ScienceDirect

Virus Research

Intranasal administration of cold-adapted live-attenuated SARS-CoV-2 candidate vaccine confers protection against SARS-CoV-2

Mohsen Abdoli [a], Maryam Shafaati [b], Ladan Kazem Ghamsari [a], Asghar Abdoli [a,c,*]

[a] *Amirabad Virology Laboratory, Vaccine Unit, Tehran 1413693341, Iran*
[b] *Department of Microbiology, Faculty Science, Jahrom Branch, Islamic Azad University, Jahrom, Iran*
[c] *Department of Hepatitis and AIDS, Pasteur Institute of Iran, Tehran, Iran*

ARTICLE INFO

ABSTRACT

With the COVID-19 pandemic globally, the ongoing threat of new challenges of mucosal infections was once again reminded human beings. Hence, access to the next-generation vaccine to elicit mucosal immunity is required to reduce virus shedding. SARS-CoV-2 retains a unique polybasic cleavage motif in its spike protein, recognized by the host furin protease. The proteolytic furin cleavage site at the junction of S1/S2 glycoprotein plays a key role in the pathogenesis of SARS-CoV-2. Here, we examined the protective immunity of a double-deleted PRRA/GTNGTKR motifs cold-adapted live-attenuated candidate vaccines as a called "KaraVac." using a hamster animal model of infected attenuated SARS-CoV-2. The KaraVac vaccinated hamsters were challenged against the wild-type (WT) SARS-CoV-2. No apparent bodyweight loss and histopathological lesions were observed in the hamsters. The establishment of sterilizing immunity was induced via stimulating a robust neutralizing antibody (NAb) response in a hamster model. Consequently, deletions in the spike sequence and inoculation into hamsters provide resistance to the subsequent challenge with WT SARS-CoV-2. We have suggested that deletion of the furin cleavage site and GTNGTKR motifs in the spike sequence attenuates the virus from the parental strain and can be used as a potent immunogen.

1. Introduction

The candidate vaccines that mimic the virus life cycle can be the best choice to protect against severe acute respiratory syndrome coronavirus 2 (SARS-CoV-2). Live attenuated vaccines (LAVs) can express endogenous viral antigens and stimulate both cellular and humoral immune responses, and are the needle- and adjuvant-free vaccines. LAVs elicit more substantial immunity than other vaccines and reduce the viral shedding, leading to less viral transmission and infection at its site of entry (Chen, 2021; Nunnally et al., 2015).

There are two motifs of the PRRA/GTNGTKR sequences, which by deletion or mutation in them, the virulence of SARS-CoV-2 is attenuated. It became one of the aspects of our interest in doing this. The COVID-19 pandemic is still raging worldwide. SARS-CoV-2 contains an additional specific polybasic cleavage motif on the S1/S2 junction of the spike protein called PRRA, which improves the pathogenicity of the virus (Zhang and Chen, 2020). In SARS-CoV-2, exclusively, the acquisition of Mut/Add in this motif has facilitated the cleavage of S1/S2 and severe infectivity in humans (Sasaki et al., 2021).

The PRRAR motif of the four amino acids, including Proline-Arginine-Arginine-Alanine, is inserted in the S1/S2 region, which has the furin cleavage site activity that increases the affinity of the SARS-CoV-2 to human cells (Davidson et al., 2020). The evolutionary pattern of the SARS-CoV-2 in the development of furin cleavage site (FCS) formation may lead to clinical signs closer to those of the HKU-1 and OC43 viruses, which have flu-like symptoms (Jin et al., 2020). The polybasic cleavage site has been found in some human coronaviruses, such as HKU1 (RRKRR) and OC43 (RRSR) and high pathogenic influenza viruses, but its role in human coronavirus is unknown. At the same time, in the avian flu virus, this motif facilitates infection in various cell types. On the other hand, this motif does not seem to play a role only in pathogenicity because in 2003, SARS-CoV, for example, which had a high mortality rate, this motif did not exist. This motif in SARS-CoV-2 is essential for establishing infection in lung cells (Wang et al., 2021a). Comparing the genomic sequence of the spike protein revealed that bat and pangolin coronaviruses were closely related to SARS-CoV-2 and contained this motif.

In contrast, other parts of the viral genome are distant apart (Chan

---

* Corresponding author at: Amirabad Virology Lab, Vaccine Unit, Tehran, Postal code: 1413693341, Iran.
E-mail address: A_abdoli@pasteur.ac.ir (A. Abdoli).

and Zhan, 2020; Pradhan et al., 2020). The cleavage of the site at the S1/S2 junction of the spike protein increases fusion with the human angiotensin I-converting enzyme 2 (hACE2) (Mengist et al., 2021). If PRRA polybasic cleavage motif was not a functional feature of the native virus and was acquired during cross-species transmission or may be inserted, it would spontaneously require high adaptations for more excellent stability and survival. There are several theories about the origin of SARS-CoV-2, all of which have remained hypothetical to this day and have not been confirmed. Still, the hypothesis that it is zoonotic is more reasonable among all (Zhang and Chen, 2020).

Depending on the hosting, coronaviruses are divided into four genera: *alpha, beta, gamma*, and *delta* coronaviruses, which NL63, OC43, 229E, and HKU1 usually infect humans. The S1/S2 junction of the spike glycoprotein of the most critical determinants is the host range, evolution and infectivity, and the varying severity of the disease. They are one of the essential goals of vaccine development because this protein contains PRRA polybasic cleavage motif, which is vital for infection and effective human transmission (Isabel et al., 2020).

Here, two motifs from the spike protein were deleted to generate the attenuated SARS-CoV-2 (which contains Del PRRA/GTNGTKR motifs called KaraVac). The second N-terminal domain (NTD) of the S1 subunit is 98% similar to the RatG13-bat virus, and the GTNGTKR motif is present in only two of the coronaviruses. This sequence is located in position 72–78 nucleotides of subunit S1. There is a 255SSG257 sequence of GTNGTKR motif. This insert is also one of the missing sequences in other coronaviruses and is only available in SARS-COV-2 and RATG13-bat and leads to cardiovascular disease and hypotension. Therefore, it seems that the insertion of the GTNGTKR motif is an evolutionary feature in SARS-CoV-2, which is related to the hACE2 through the S1-C-terminal domain (CTD) on one side and to sugar (Neu5, 9Ac2) and protein (vascular cell adhesion molecule-1 / VCAM-1) receptors via S1-NTD. SARS-CoV-2 has helped better adaptation and escape from the host's immune system by binding to hACE2 and non-hACE2 receptors (Behloul et al., 2020; Hikmet et al., 2020).

Preliminary analyzes showed that S1/S2 junction was under selective pressure because SARS-CoV-2 was circulating in the human population. Under intense selective pressure, the unique furin cleavage site causes the highest infectivity in humans. In previous studies, due to repeated passages in the Vero cell line, the adaptive function of the SARS-CoV-2 is lost, and the potential of Del-Mut strains should be investigated as a seed for live-attenuated vaccines (Chan and Zhan, 2021). We have shown that deleting (Del) the two sequences from the spike protein at the S1/S2 junction and S1-NTD of SARS-CoV-2 is attenuated in its ability to cause infection in this SARS-CoV-2 animal model. We used this attenuated virus as a candidate for a live-attenuated vaccine and evaluated their immunogenic potential in this scope.

2. Materials and methods

2.1. Generation of live-attenuated SARS-CoV-2

According to WHO guidelines, the SARS-CoV-2 viruses were serial passaged several times on Vero E6 cells (World Health Organization, 2020). The Vero cells (ATCC# CCL81) were seeded into a T-25 flask in Dulbecco's modified Eagle medium (DMEM) (Bio Idea) supplemented with 10% fetal calf serum (FBS) (Sigma, Germany), 100 IU/ml penicillin, and 100 mg/ml streptomycin (Pen/Strep) (Invitrogen), and incubated at 37°C in the presence of 5% CO2 incubator. After reaching 90% confluency, the growth medium was replaced. In the next step, Vero E6 cells were infected with 0.05 MOI of the virus, and 72 h post-infection, it was harvested (Abdoli et al., 2013). When the cytopathic effect of the virus was mild compared to the wild-type, its sequence was determined (using the Sanger method).

2.2. Cold-adaptation of SARS-CoV-2

The cold-adapted SARS-CoV-2 was generated via serial passages of SARS-CoV-2 in the Vero cells at a suboptimal temperature from 35°C to 25°C. To determine the temperature sensitivity phenotype, the titers of the cold-adapted SARS-CoV-2 were assayed in the Vero cells at 33°C, 39°C, or 41°C [with a modification from Seo and Jang 2020]. The cold-adapted SARS-CoV-2 grew at 33°C and 39°C, respectively, but failed to replicate at 41°C. In contrast, wild-type SARS-CoV-2 replicated well at 33°C, 39°C, and 41°C.

2.3. Virus characterization

The whole genome of the virus was sequenced after attenuation and cold adaptation. Next, the cold-adapted SARS-CoV-2 structure was evaluated through electron microscopy that grids were analyzed using a transmission electron microscope [sample preparation: negative staining PTA 2%, uranyl acetate 1%] (TEM: PHILIPS, EM208S, 100KV, NEDERLAND). The virus growth kinetics was assayed via 50% tissue culture infective dose (TCID50) up to 120 h post-infection (hpi).

2.4. Virus neutralization assay (cVNT)

The conventional virus neutralization test (cVNT) was used to evaluate the sera collected from hamsters and determine the level of functional antibodies produced against SARS-CoV-2. Briefly, 50µL of twofold serial dilutions of heat-inactivated sera (at 56°C for30 min; as triplicates) were mixed with 50 µl of 100 TCID50/mL of SARS-CoV-2 in Dulbecco's Modified Eagle Medium (DMEM) free FBS and incubated for 1h at 37°C. The virus/serum mixtures were then transferred onto monolayers of Vero E6 cells in 96-well plates for 60 min at 37°C. The supernatant was removed at 1h after infection; the infected cells were washed twice with PBS1X and incubation in DMEM for 72 h at 37°C in a 5% CO2 incubator (Abdoli et al., 2021; van Tol et al., 2020).

2.5. Antibody measurement

The serum anti-SARS-CoV-2 IgG (anti-spike IgG) levels in KaraVac-vaccinated hamsters were evaluated using indirect ELISA 4-weeks post- immunization. The anti-SARS-CoV-2 IgG antibody titer was assayed through an enzyme-linked immunosorbent assay (ELISA: PishtazTeb) (Abdoli et al., 2021). Briefly, 96-well plates were coated with the purified RBD protein (10 µg/mL) in PBS (pH 7.2) overnight incubation at 4°C. Then the plates were washed three times with PBS containing 0.05% Tween 20 (PBST) and blocked with 5% skim milk in PBS at 37°C for 1.5 h. After the washing, serial dilutions of sera in PBS were added to the plates and incubated at 37°C for 1.5 h. Horseradish peroxidase-conjugated anti-hamster IgG antibody (ab6892) at 1/10000 dilution was added to the wells, and after washing with PBST, the plates were incubated for 1.5 h at 37°C. Colorimetric detection was performed using 100 µL 3,3′, 5,5′-Tetramethylbenzidine (TMB, Sigma) as substrate after washing and incubation for 30 min at RT. The reaction was stopped with 50 µl H2SO4 (2 N), and absorbance was measured at 450 nm using an ELISA reader.

2.6. Immunization and challenge

An animal model of the Syrian golden hamster was used to evaluate the KaraVac features *in vivo*. Studies have shown that this animal model is suitable for examining the characteristics of COVID-19 infection. Sixty 7-8-week-old golden Syrian hamsters were divided into six groups, as a Table 1. The hamsters were immunized via the intranasal route. After 21 days, the animal sera were collected, and antibody level was measured. On the day of 28, the animals were anesthetized intraperitoneally with ketamine and xylazine and then challenged intranasally with 200 µl of wild-type SARS-CoV-2 (10^6 TCID50/ml). Bodyweight and disease

Table 1
Grouping of vaccinated hamsters with KaraVac (LAV) in the challenge wild-type SARS-CoV-2[***].

Target groups	Grouping	Injection dose (VP[*])	Total injection volume (µl)	Delivery route	Number of injections	Number of animal model (Hamster)
1	Control	PBS buffer[**]	200	Intranasal	1	5
2	Test	10	200	Intranasal	1	5
3	Test	10^2	200	Intranasal	1	5
4	Test	10^3	200	Intranasal	1	5
5	Test	10^4	200	Intranasal	1	5
6	Test	10^5	200	Intranasal	1	5

[*] To the best dose-finding of viral particles (VPs).
[**] Phosphate-buffered saline (abbreviated PBS).
[***] The LAV was injected intranasal into the hamsters. The total injection volume was 200 µl, and the injection volume into each nasal cavity was 100 µl.

symptoms were checked daily. Lung tissues in the virus-challenged hamsters were collected on the seventh day post-infection and processed for hematoxylin and eosin staining (H&E). The histopathology of the lung tissue for viral replication was performed by H&E and analyzed by light microscopy as in a prior study to evaluate the changes of the virus (Chan et al., 2020). On day six, lung tissues were collected from hamsters from each group to assess virus titers by TCID50 using Spearman-Karber methods (Miller and Ulrich, 2001). The study protocol was approved by the Ethical Committee of Tabriz University of Medical Sciences.

2.7. SARS-CoV-2 quantification in lungs after challenge

The lung homogenates were clarified through centrifugation at 4000 g for 10 min to remove cell debris, and the supernatants were then stored at −80°C until the assay was performed. Vero cells with 80 confluences in 96-well plates were infected with serial ten-fold dilutions of clarified lung samples in DMEM. After 72 h of incubation at 37°C in a 5% CO2 atmosphere, the culture was observed for the cytopathic (CPE) of SARS-CoV-2. The viral titer in each lung specimen was calculated by the Karber method (Miller and Ulrich, 2001) and expressed as the 50% tissue culture infective dose (TCID50).

2.8. Statistical analysis

All experimental data were analyzed with at least three independent t-test and Mann- Whitney tests, ANOVA ± SD, and draw charts were performed using Graph Pad prism 9. Any differences were assessed using a t-test, and **$0.01 < P < $*$0.05$ was considered significant.

3. Results

3.1. The properties of generation KaraVac vs. wild-type SARS-CoV-2, showing deletion of PRRA & GTNGTKR from the spike protein

We used the whole genome WT SARS-CoV-2 in the NCBI database (GenBank accession No. MN985325.1) by deleting 30 and 27 nucleotides at the S1/S2 junction site (PRRA motif) and the S1-NTD site (GTNGTKR motif), respectively, both of which were located on the spike protein (sequence alignment of nucleotides shows that this X-bp deletion is located at spike protein SARS-CoV-2). In this way, we logically designed a potential candidate for a live-attenuated virus/ vaccine against the wild-type SARS-CoV-2 (Fig. 1).

3.2. Electron microscopy analysis of attenuated SARS-CoV-2 morphology

We analyzed them under electron microscopy (EM) to better understand the status of attenuated SARS-CoV-2 virions. The morphology of attenuated SARS-CoV-2 particles was identified after detailed examination by electron microscopy. Relative size is shown by the size bar in the lower corner of the image (100 nm) (Fig. 2).

3.3. Propagation of attenuated SARS-CoV-2 as a vaccine candidate

A schematic representation of WT SARS-CoV-2 is shown in Fig. 1A. Part of the gene sequences coding S protein was deleted to construct the LAV candidate (Fig. 1B and C). We were generated as the attenuated SARS-CoV-2, which lacked 57 nucleotides compared to the wild-type SARS-CoV-2 in its spike sequence. The attenuated virus was passaged
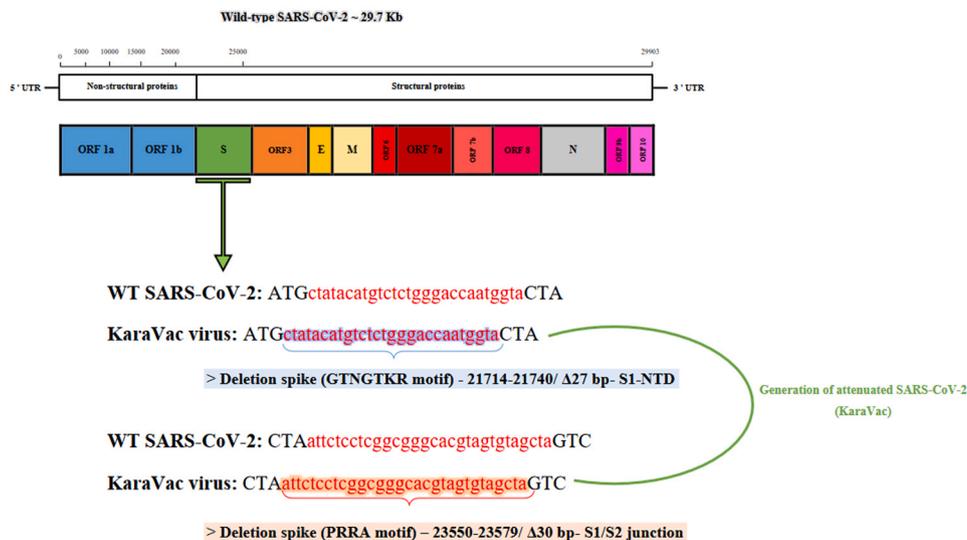
Fig. 1. Schematic illustration of the genome organization Wild-type SARS-CoV-2 and how to generate KaraVac. (A) The Wild-type SARS-CoV-2 genome organization and spike protein, (B) Generation of attenuated SARS-CoV-2 from deleting S1-NTD of the spike protein (GTNGTKR motif/ deletion 27 bp), (C) Generation of attenuated SARS-CoV-2 from deleting the furin cleavage site insertion of the spike protein (PRRA motif/ deletion 30 bp).
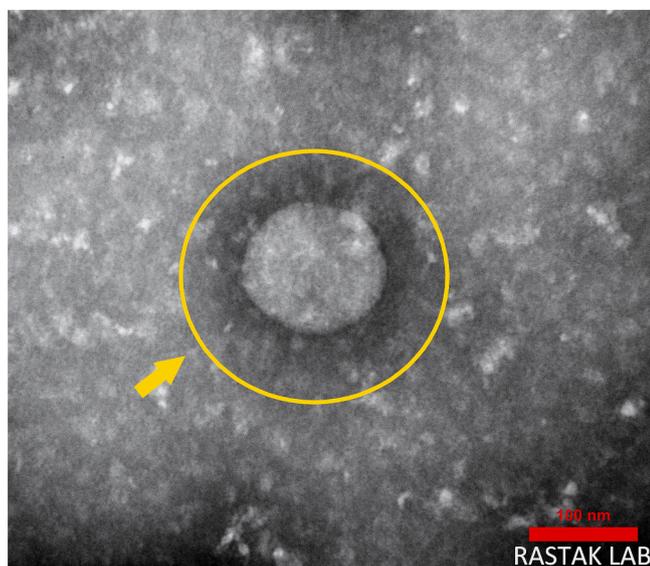
Fig. 2. Complementary analysis by Transmission electron microscopy (TEM). (A) Electron microscopy of attenuated SARS-CoV-2 infected Vero cells that coronavirus particles highlighted (yellow ring). Viral particles remained in cell culture (CPE). Carbon Formvar Coated 300 Mesh Copper Grids, supplied by Agar Scientific in TEM.

in Vero cells to produce the cytopathic effect (CPE) (Fig. 2). The attenuated virus grew well on Vero cells. We examined the KaraVac growth (attenuated virus) under conditions of cold-adaptation (from 37°C to 25°C). Robust growth of KaraVac occurred at 72- and 96 h post-infection (hpi) in Vero cells, which was approximately equal to 10^7, confirming that KaraVac can be quickly produced and replicated on a large scale. Maximum attenuated virus production occurred on the third- and fourth days post-infection (10^7 TCID50) (Fig. 3). As expected and based on published evidence, the potential is attenuated with furin cleavage site removal, resulting in reduced direct cell to cell transmission in the infected host in contact with others (less viral shedding). Combining the results of Electron Microscopy and a graph of attenuated virus replication showed that with the loss of the two mentioned motifs, efficient replication increased in Vero cells, and increased proliferation was associated with more CPE at 72 and 96 hpi. The amount of virus
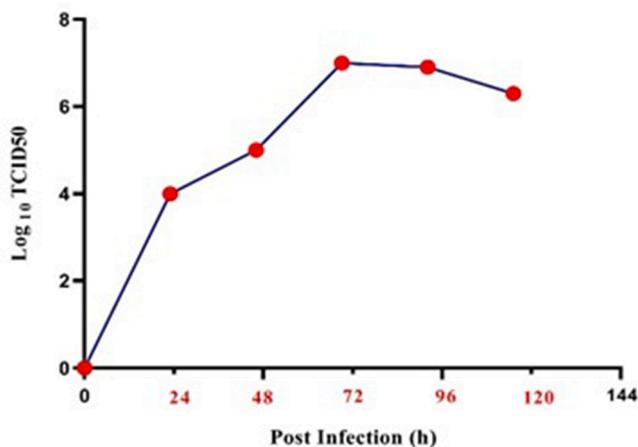
concentrated per mL capable of producing cytopathic effect (CPE) in 50% of inoculated Vero cells was calculated using the Karber formula. The infectivity titer of the attenuated virus was reported on TCID50/ mL. The mRNA and viral vector vaccines encode only the spike protein, restricting the immune response against this viral antigen. Live-attenuated vaccines can elicit immunity to several viral antigens, enhancing the chances of protection. It should note that intranasal administration of attenuated SARS-CoV-2 can stimulate secretory IgA (sIgA), which may increase the neutralization of SARS-CoV-2, and is considered a potential benefit.

3.4. Evaluation of the humoral immune response of KaraVac

3.4.1. Assessing antibody neutralization of KaraVac

We evaluated the impact of X-nucleotides deletion in the two mentioned motifs from the spike protein on the neutralization of attenuated SARS-CoV-2 (KaraVac) to determine efficient immunogenicity. The results demonstrated that NAbs have a high affinity for neutralizing the virus in Vero culture (according to the cVNT approach). Immunization of hamsters with an intranasal dose of KaraVac resulted in a high protective immunity against 10^5 viral particles (TCID50/ mL) in the wild-type SARS-CoV-2 challenge compared with the control group. The neutralizing titer was estimated by the dilution number of 50% protective condition (Fig. 4).

3.4.2. KaraVac vaccine stimulate high levels of RBD antibodies

The results showed that anti-SARS-CoV-2 IgG boosted hamsters vaccinated with KaraVac ($P < 0.01$, groups 5 and 6). The anti-SARS-CoV-2 IgG was highly significant in hamsters immunized with the challenge 10^4 and 10^5 purified inactivated VPs (Ag). Unlike WT, the KaraVac inoculation induced robust anti-S1 RBD-specific NAb responses

Fig. 3. Viral titer from Vero cells infected with attenuated SARS-CoV-2. Vero cells were infected with KaraVac. Results reported as log 10 of TCID50 culture medium. All experimental data were analyzed with at least three independent t-test and Mann- Whitney test. Statistical analyses and draw charts were performed using and Graph Pad prism 9 and **$0.01 < P < $*$0.05$ was considered as significant.

| GMT ratio (SD): | 0 | 57.6 | 179.2 | 358.4 | 614.4 | 819.2 |

Fig. 4. KaraVac alters SARS-CoV-2 serum neutralization (neutralization activity against the attenuated virus). The virus neutralization assay (VNT) results in the hamsters vaccinated with KaraVac, which was reported as GMT (geometric mean of neutralizing antibody titers), showed that the neutralizing serum titers up 1/256 in groups 4, 5, and 6 can neutralize the attenuated virus by post-one inoculated/ intranasal- 200 µl - (specifications in Table 1). In the three groups mentioned, the challenge with WT direct inoculation was 103, 104, and 105, respectively, which occurred in the 105 highest titers of serum neutralization against the attenuated virus. The symbol of the C group was the control group, and the symbol of T was the test group (Table 1). The GMT of all groups is shown at the bottom of the X-axis, and seroprotective of all six groups is 338.113. All experimental data were analyzed with at least three independent t-test and Mann- Whitney test. Statistical analyses and draw charts were performed using and Graph Pad prism 9 and **$0.01 < P < $*$0.05$ was considered as significant. Ns: not significant. Error bars represent mean ± SD ($n = 6$).

(anti-spike IgG) (Fig. 5). That means humoral immunity post-infection with the attenuated virus causes a rapid and robust response. The post-infection neutralizing titers were significant in hamsters previously vaccinated with the KaraVac. The results of Figs. 4 and 5 show that vaccine-elicited NAbs induced adequate immunity in hamsters after challenge with wild-type SARS-CoV-2.

3.5. Evaluation KaraVac's attenuating characteristics in vivo

According to the specifications of Table 1, the hamsters were vaccinated with KaraVac, and they have encountered a wild-type SARS-Cov-2 challenge. The challenge was carried out with 10^6 TCID50 of the WT. The hamsters' weight change was followed for seven days post-infection to evaluate the hamsters' safety. Six groups of 5 hamsters were inoculated with 10^6 VP in the control group (WT/ PBS) and the test group (KaraVac) for seven successive days for body weight changes. Compared to the WT, the KaraVac -vaccinated hamsters did not experience significant body weight change seven days post-infection (dpi). Following the challenge with the wild-type SARS-CoV-2, the test group consistently maintained their body weight from day 1 to day seven post-infection. On day four post-infection, the peak weight loss was nearly 20% declined but again, from the next day until day seven remained close to their starting weight (Fig. 6). T-test showed that weight changes between the test (KaraVac) and control (WT/ PBS) groups were significant ($P < 0.05$).

3.6. Lung histopathology in hamsters in vivo

Histopathological samples were collected on day seven post-challenged. The KaraVac live-attenuated virus showed no apparent lung histopathological changes in hamsters compared to wild-type SARS-CoV-2. A difference is that WT causes extensive destruction of the alveolar wall, necrosis of epithelial cells in the lungs of infected hamsters, and bleeding of the alveolar space compared to KaraVac. They have marked with arrows in the figures (Fig. 7).
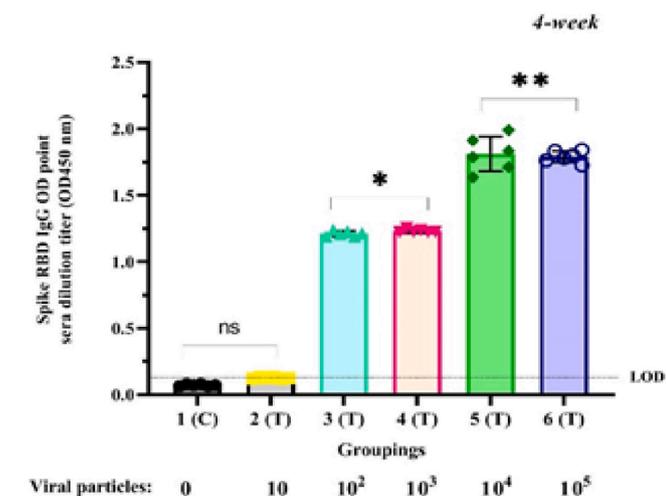
Fig. 5. The KaraVac effect on hamsters (anti-S1 RBD-specific IgG titers). Levels of the receptor-binding domain (RBD)-specific IgG antibodies in sera collected 4-weeks post-infection were determined. Primary infection with KaraVac and WT elicited neutralizing antibodies in the serum and potentiated the re-challenge of this activity. Hamsters (groups 3 to 6) inoculated with KaraVac produced NAb titers at similar levels. All experimental data were analyzed with at least three independent t-test and Mann- Whitney test. Statistical analyses and draw charts were performed using and Graph Pad prism 9, and **$0.01 < P < $*$0.05$ was considered as significant. Ns: not significant. Error bars represent mean ± SD ($n = 6$). LOD: level of detection.
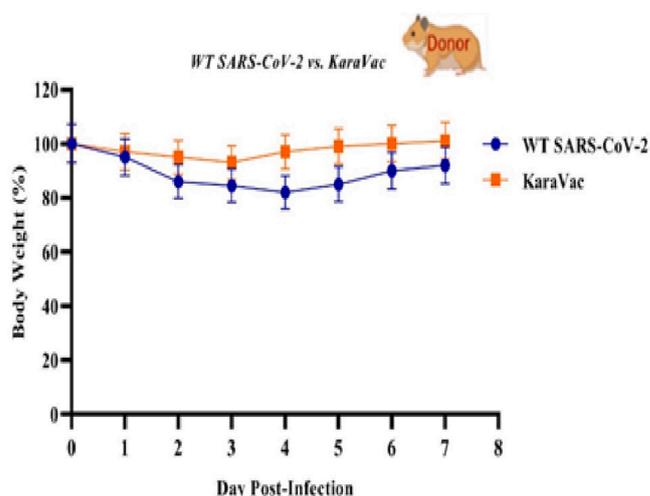
Fig. 6. Safety of KaraVac in hamsters (Body weight changes of hamsters). The weight of hamsters was measured daily for seven days post-infection. Wild-type SARS-CoV-2-infected hamsters experienced slight body weight loss from day 1 to 4, but this condition stabilized from day four post-infection. In contrast, KaraVac-vaccinated hamsters did not experience noticeable body weight loss during these seven days. Weight changes were significantly different between KaraVac- test group: orange and WT/PBS–control group: blue ($n = 7$ to 6 groups for KaraVac and WT/PBS, $P < 0.05$).

3.7. Measuring the efficacy of KaraVac in challenge studies

To KaraVac be more effective in challenging wild-type SARS-CoV-2, our question was whether immunization with KaraVac in hamsters would protect them from being challenged with the WT? After immunization with KaraVac, hamsters were challenged with WT SARS-CoV-2. Hamsters vaccinated with KaraVac could maintain their body weight post-challenge (Fig. 6). Six-day post-challenge, their lungs were harvested (on day 8). Infectious titer was measured based on TCID50/ mL. Infectious titers in WT challenge in KaraVac-vaccinated hamsters were declined in groups 5 and 6 compared to the control group and group 4 of the four-$\log_{10}$ ($P < 0.01$), indicating vaccine efficacy (Fig. 8). Analyses of virus replication in the lung tissue of challenged hamsters showed that KaraVac inhalation provides sterilizing immunity against following challenges with the WT SARS-CoV-2. The KaraVac conferred protection, and there was no report of the vaccine-enhanced disease in the challenge.

4. Discussion

The COVID-19 pandemic led to the development of various vaccines with different platforms in a short and uninterrupted period. But these advances have not yet been made to the proper SARS-CoV-2 mucosal vaccines. Thanks to intranasal mucosal vaccines, the immune response is stimulated at the primary site of infection, and sterilization immunity is enhanced by triggering the response of local secretory antibodies and cellular immunity. Therefore, the value of mucosal vaccines is immunologically high, their delivery route is more accessible, and there is no need to challenge the safety of the adjuvant. In addition to the independent function of mucosal vaccines, their prime-booster strategies should also be considered a promising option (Lavelle and Ward, 2022).

Most available vaccines are administered by injection. The mucosal vaccines can exceed parenteral vaccination approaches in evoking protective mucosal immune responses that blockade infection or transmission. The nature of the infection in designing mucosal vaccines has been considered (Okamura and Ebina, 2021). Robust mucosal cellular and humoral immune responses can elicit sterilizing immunity by inhibiting Spike SARS-CoV-2-hACE2 binding. One of the aims of our
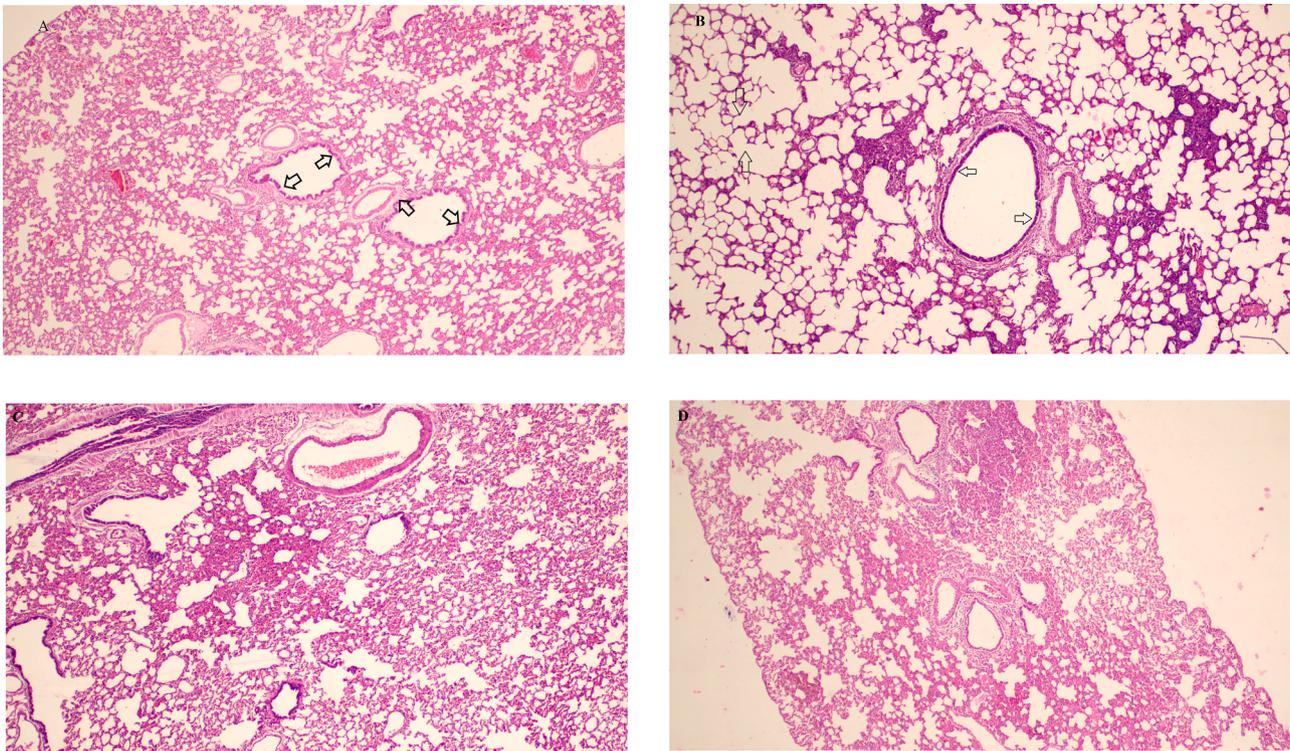
Fig. 7. Histopathological analysis of lung tissues from hamsters immunized with KaraVac live-attenuated virus and challenged with WT SARS-CoV-2. The lung tissues histopathology of hamsters at 7 dpi was stained with H&E (A, B, C) × 100. (A) Analysis of the lung tissue challenged with WT SARS-CoV-2 shows that the hamsters immunized with KaraVac elicited post-challenged sterilizing immunity. Hamsters immunized with KaraVac experienced mild alveolar infiltration, and no intricate histopathological changes were observed in their tissues, (B) Analysis of the hamsters' lung tissues that received placebo and then challenged with WT SARS-CoV-2: revealed extensive alveolar collapse, detachment of the bronchial epithelial layer, and more extensive lung tissue damage in hamsters infected with WT (arrow), (C) Analysis of the lung tissues of hamsters that neither KaraVac received nor with the WT SARS-CoV-2 challenged. This group only received PBS. (The A group intranasal (i.n.) was immunized with the KaraVac virus and then challenged with WT [as a test group]. The B group received a placebo, and then i.n. were challenged with WT [as a positive control]. The C group only received PBS without being challenged with WT or immunized with KaraVac [as a negative control]), (D) The hamsters' lungs vaccinated with KaraVac alone showed no noticeable histopathological changes.
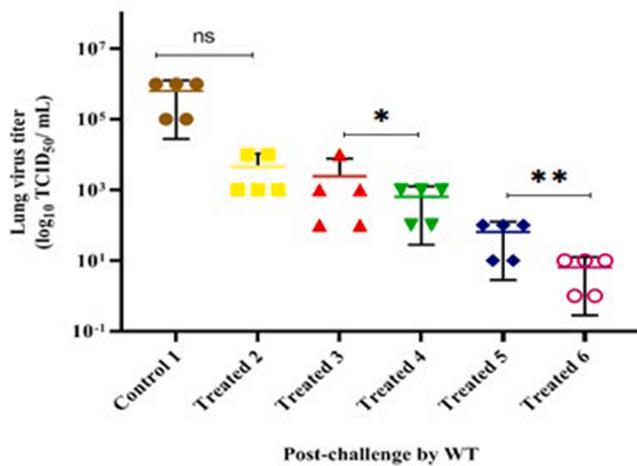
Fig. 8. KaraVac efficacy. KaraVac immunization protection against WT SARS-CoV-2 challenge in hamsters. Infectious titers were measured by TCID50/mL and expressed as log10 of viral particles/mL of lung tissue. All experimental data were analyzed with at least three independent t-test and Mann- Whitney test. Statistical analyses and draw charts were performed using, and Graph Pad prism 9 and $**0.01 < P < *0.05$ was considered as significant. Ns: not significant. Error bars represent mean with 95% CI ($n = 5$).

study was to pave this challenging track.

The change in SARS-CoV-2 proteins compared to previous coronaviruses is one of the major reasons for the shift in host preference and different pathogenicity. According to this approach, we also tracked changes in the level of spike (S) protein SARS-CoV-2. There are four distinct insertions in the protein spike SARS-CoV-2 compared to SARS-CoV's closest relatives. Our sequencing showed that the inserts in the wild-type of SARS-CoV-2 are appealing conserved, which means that the inserts are specific to SARS-CoV-2, which causes its survival and high infectivity in lung cells. Any changes in S protein cause a shift in host tropism and a virus-host specificity. This is also due to the tendency of SARS-CoV-2 towards human cells, which is due to the mutation and evolution of the virus compared to previous coronaviruses. These insertions also cause a high affinity of the virus to host cell receptors.

To create a live-attenuated candidate vaccine against SARS-CoV-2 (deliverable intranasally), we gradually cold-adapted WT SARS-CoV-2 from 35°C to 25°C. A temperature of 25°C was chosen to study the vaccine's efficacy, and the virus at this adaptive temperature had known as KaraVac. Features of this novel double-deletion live-attenuated virus can mention the most important ones that make it a candidate for a LAV.

The KaraVac has more robust growth in the Vero-E6 cell line than the wild-type virus, and its fitness is better in this cell line. Spike protein processing was also reduced compared to WT. Del PRRA in KaraVac, like the SARS-CoV-2, has almost full-length S protein (85%), with the lowest processing rate between S1/S2 junction (14.5%). The results show that following infection in Vero cells, S protein processing is mainly performed by the furin cleavage site. The N-terminal domain of the S1 subunit SARS-CoV-2 (GTNGTKR motif) is 98% similar to the RatG13-bat coronavirus (Behloul et al., 2020). The GTNGTKR motif is present in only these two coronavirus viruses. This sequence is located in the 72–78 position of the S1 subunit. Alignment of this sequence in the database

found that other proteins in other organisms also have this motif. The first is the VP1 from the Mengo virus; another is in the tail spike bacteriophage protein CBA120. The Mengo virus can bind to the VCAM-1 receptor (vascular cell adhesion molecule-1) and enter the cell. This receptor is restricted to endothelial cells and is upregulated under cytokine stimulation.

Given that large amounts of cytokine cascade are produced by stimulation of SARS-CoV-2 and underlying cardiovascular diseases such as hypertension and coronary heart disease are major contributing factors resulting from SARS-CoV-2 mortality, the removal of the GTNGTKR motif clears this negative trait (this motif is essential in autoimmune diseases, inflammatory diseases or infections). GTNGTKR motif can detect the sugar receptor (Neu5, 9Ac2 receptor) that binds to the bovine coronavirus. SARS-CoV-2 has evolved to bind more strongly to the hACE2 receptor through S1-CTD and sugar or protein receptors through the S1-NTD. Acquisition of the GTNGTKR motif enables the SARS-CoV-2 to bind to receptors non-hACE2. Deleting this motif can block the virus from entering the cell.

Many previous studies, such as Johnson et al. (2021), Wang et al. (2021a), and Lau et al. (2020); were focused on single-deletion at the furin cleavage site (S1/S2 junction). Their results showed that the lack of the furin cleavage site plays an essential role in the evaluation and activity of NAbs because removing a PRRA motif in WT SARS-CoV-2 leads to low-grade (poor) infection. In addition to the PRRA motif's mutation, another deletion was performed in the GTNGTKR motif, which novelized the virus with double-deletions and reduced the probability of virus recombination with circulating one. Removing them weakened the infectivity of the resulting virus and attenuated its replication *in vivo*.

The COVID-19 pandemic sparked a strong interest in vaccine makers for intranasal vaccines. Researchers have been trying to potentially use inhaled vaccines against infections that affect the upper respiratory tract for several years. We believe that the best defense occurs at the entrance gate. The vaccine enters the upper respiratory tract and lungs through the nose to stimulate mucosal immunity, which cannot be induced by intramuscular injection (Xi et al., 2021). Today, there are more studies on the induction of mucosal immunity by intranasal and parenteral routes, the most important of which are mentioned. In a more specific study by Oh et al. (2021), secretory IgA (sIgA) was crucial in developing lung antiviral immunity. Still, the particular cells that produce mucosal sIgA and their physical location are unclear. They showed that the proliferation of respiratory viruses such as flu, whether from previous infection or vaccination, elicited sIgA in the intranasal routes rather than injections (production of IgA through lung-resident memory B cell, plasma cells). These findings add to previous, growing evidence that mucosal vaccination strategies are more effective in promoting mucosal immunity against respiratory pathogens such as SARS-CoV-2. While Clements and Freytag (2016) showed that a mucosal immune response induction would also occur post-parenteral vaccination, the pattern of stimulation of an appropriate protective mucosal response depends on the vaccine design and delivery strategy.

Other reports show that mRNA vaccines induce a mucosal immune response (antigen-specific nasal and salivary) and produce spike-specific IgG and IgA (Chan et al., 2021; Guerrieri et al., 2021; Ketas et al., 2021). Overall, mucosal vaccination elicited a double layer of immunity, both systemically and at mucosal surfaces. As a result, LAV vaccines are the most potent vaccines that mimic the entry route of the SARS-CoV-2 into the body and act as self-replication, which our study supports. For these reasons, we suggested a LAV COVID-19 candidate (KaraVac). In KaraVac, deletion occurred to spike protein's coding region of two motifs, PRRA/GTNGTKR. This re-coding in KaraVac genomic sequence resulted in the deletion of 30 and 27 nucleotides, one at the polybasic furin cleavage site (S1/S2 junction) and the other at S1-NTD in the spike protein. The virus was generated significantly attenuate, and it was considered a non-optimized LAV candidate against challenging the wild-type SARS-CoV-2 strain.

Due to continuous antigen stimulation in LAV, the elicited immune response is far greater than the WT strain and provides ample time to develop memory immunity. Thus, an abroad immune response is induced against the viral antigen. Even when antigenic drift, the attenuated SARS-CoV-2 as a LAV keeps its efficacy among the human population. We hope to be attenuated SARS-CoV-2 is used as a LAV because the attenuated virus has the rare potential to revert to a pathogenic state and cause disease in vaccines or their contacts. Viral shedding is less common with live-attenuated viruses. Therefore, served as a mass immunization campaign (Yaqinuddin et al., 2021), which was consistent with the results of our study. This study targeted two sequences on the spike protein SARS-CoV-2 to evaluate the impact of the deletion on immunogenicity. Initially, a viral stock was prepared during multiple-repeated passages of wild-type SARS-CoV-2 in the Vero cell line. After the passages, the isolates were examined for plaque purification, and the whole-genome sequencing of the isolates derived from plaques was analyzed. After applying extreme conditions, to evaluate the duration of pathogenicity, viral replication, and the stability compared to the wild-type strain, we deleted 30 nucleotides from the polybasic cleavage site at the S1/S2 junction as a called PRRA motif (23550bp- 23579bp, Δ30bp) and another 27 nucleotides from the GTNGTKR motif at S1-NTD (21714bp- 21740bp, Δ27bp). Both of these motifs are on the spike SARS-CoV-2. Notably, deletion of the furin cleavage site in the spike SARS-CoV-2 resulted in more excellent safety to the vaccine strain, and a high attenuated virus of SARS-CoV-2 was generated, which we called KaraVac. This new virus had acquired a suitable adaptation due to extreme conditions and frequent passages in the Vero cells. It was then confronted under conditions cold of adaptation and a change in the temperature range from 37°C to 25°C. Finally, pathogenicity was assessed in the animal model of hamsters, a related small animal model for COVID-19. We obtained some interesting results from the wild-type strain challenge: the ability to reduce disease in hamsters was reduced to the point where no evident virulence was observed. We used KaraVac as a live-attenuated vaccine (LAV) candidate to immunize hamsters, which showed complete protective immunity in a challenge with the wild-type strain and triggered a robust development response to neutralizing antibodies (NAbs). The deletion PRRA/ GTNGTKR is a live-attenuated SARS-CoV-2 vaccine seed that induces RBD specific-NAbs. Weight loss was not seen in the animal model of the hamsters (no complication of intricate histopathology). Except for two sites deletion, the KaraVac and WT SARS-CoV-2 gene sequences are equal, supplying that all viral proteins can be involved with the host immune system of the vaccine.

Since there was no history of human vaccination against SARS-CoV-2, COVID-19 vaccine manufacturers' concerns are whether all current vaccine strategies can establish long-lasting immunity to prevent and reduce COVID-19 infection and relieve its severity pathogenicity (Kyriakidis et al., 2021; Zhang and Chen, 2020). This study showed that the KaraVac virus-induced an innate immune response different from that which occurs with the wild-type strain in the animal model. After inoculating a single dose of the KaraVac virus into the hamster and its exposure to the wild-type strain, it significantly promoted the arrival of a virus-neutralizing antibody response as robust than resulted from a WT infection. Intranasal vaccines are a promising approach to inhibiting SARS-CoV-2 due to the development of mucosal immunity. Intranasal vaccine research for COVID-19 has focused on viral vector or protein subunit platforms, all of which require appropriate mucosal adjuvants and delivery systems against mucosal barriers to enhance the immune response. However, they have led to robust protective immunity in animal models, which can be improved in clinical trials (Alu et al., 2022). Based on previous studies, we used the cold-adapted LAV platform to create KaraVac because the scale pan of intranasal vaccines is weightier than those of intramuscular vaccines, which sterilize mucosal and systemic immunity prevents further transmission and infection of the virus.

Wu et al. (2021) examined the safety and immunogenicity of an Ad5-nCoV vaccine (aerosol inhalation) in individuals ≥18 years. The Ad5-nCoV contained an incomplete replication Ad5 vector that could

express the full-length spike gene of the WT SARS-CoV-2 and was used in liquid formulations for intramuscular and aerosol administration. Their results on the 28th-day post the last vaccination showed that the geometric mean of neutralizing antibody titers SARS-CoV-2 is seroprotective. Secondly, intramuscular vaccination produces a higher RBD-binding IgA/IgG concentration than the aerosol vaccination, but the NAb titers of SARS-CoV-2 in the aerosol vaccination are similar to intramuscular immunization. In response to these conditions, it should be noted that the safety profile of aerosol vaccination is different from that administered intramuscularly. Still, the immune responses are similar to those of the recombinant protein or mRNA COVID-19 vaccines. These findings were consistent with our overall goals of stating that different pathways of vaccination produce different antibodies that are stimulated in aerosol vaccination than in intramuscular vaccination, with more NAb titers than total antibodies. What is certain is that some mucosal vaccines (like nasal spray flu vaccine) develop a similar protective effect even if the antibody titers are lower than the intramuscular administration (Coelingh et al., 2015; Hoft et al., 2017).

HKU1, OC43, 229E, and NL63 strains are common cold causes of coronaviruses. While the primary and intermediate host for SARS-CoV-2 has not been determined with certainty, it has contaminated human cases through cross-species transmission (Ma et al., 2020). Analysis of our study showed that attenuated virus is stable. It also enables the acquired function of wild-type SARA-CoV-2 to replicate in the non-permissive cell line. On the other hand, the crucial role of additional proteases for the virus to enter environments where extreme conditions do not exist should be investigated because circulating coronaviruses associated with the common cold lack the S1/S2 junction, so if SARS-CoV-2 ever evolves into a fully human virus, it remains to be seen which mutant is the virus's final form, highlighting the importance of evaluating deleted attenuated for vaccine production? In a similar and new study by Wang et al. (2021b), the COVI-VAC vaccine was developed by codon-pair deoptimization and furin cleavage site deletion. By re-coding and optimizing the codon-pair in this vaccine, 238-point mutations were introduced. They deleted the furin cleavage site from the spike protein SARS-CoV-2 for more excellent safety, but the rest of the COVI-VAC amino acid sequence was the same as that of parental SARS-CoV-2. The COVI-VAC was sensitive to temperature *in vitro* but grew at the permissible temperature, the lung pathology was milder, and the weight of hamsters immunized with the COVI-VAC was lower than in the WT. Also, after the challenge with wild-type virus, the viral titers of lung challenge decreased, and the neutralizing antibody titers increased. The study found that SARS-CoV-2 without the furin cleavage site (this region helps the virus escape the innate immune response) was attenuated in small animal models. Its transmission capacity to the host was significantly reduced. With these arguments and past literature studies (Johnson et al., 2021; Lau et al., 2020), we also decided to remove this site to create a KaraVac. The difference is that the attenuated phenotype of the KaraVac strain was a combination of double-deletion PRRA/GTNGTKR motifs, which is an innovative aspect of this study compared to the previous research.

Based on this study, we suggest that the formulation and route of administration of next-generation vaccines to control the COVID-19 pandemic would be better by intranasal because this route of delivery of the vaccine causes severe stimulation of memory cells mediated B/ T cells and secretory IgA. All of these play a significant role in the viral shedding in the occurrence of re-infection, and this is important for intranasal LAV. After all, the live-attenuated virus elicits mucosal immunity in the upper respiratory tract and antigen delivery to the site of infection, which is their high score because it causes them to have less viral shedding than injectable vaccines. Our data supported this discussion. Here's why intranasal vaccines are more effective than other current vaccination platforms for COVID-19: LAVs can bypass risks such as antibody-dependent enhancement (ADE). According to the Chen (2021), if a high-efficacy-safe LAV for COVID-19 is introduced worldwide before August 2022, it could destroy one or two recent waves of the SARS-CoV-2 pandemic, provided the severity of seasonal COVID-19 is the same as other respiratory illnesses and 50% of the world's susceptible population is vaccinated. Thanks to technologies such as cold-adaptation in LAV, the transmission and virulence to humans is prevented, i.e., the transmission of LAV as a live-attenuated virus to humans are minimized, and the risk of disease recurrence is decreased (less viral shedding). The attenuated virus replicates well *in vitro* cell culture. Finally, the safety of LAVs can be boosted by intramuscular injection or oral administration to eliminate the risk of vaccine-induced pneumonia, like in the case of adenovirus immunization in American soldiers. Eventually, along with the LAVs, the NAbs turn them into a live-immune complex to provide protection immediately post-vaccination (Maassab, 1999).

This study led to the generation of a cold-adaptive virus called KaraVac. One of the deletions occurred in the PRRA motif within the S1/S2 junction. The other occurred upstream of the S1 subunit of one of the spike proteins (S1-NTD). Characteristics of the KaraVac virus showed no obvious pathogenicity to the wild-type strain in hamsters. Appropriate protective immunity was induced against infection with the wild-type strain in hamsters. We found that by removing the furin cleavage site and the GTNGTKR motif, the KaraVac virus proliferated with a low cytopathic effect. Still, the point to note is that we believe that the circulating variants of SARS-CoV-2, with their increasingly adaptable features, will continue to in human populations (Assessment, 2021).

5. Conclusion

With the lapse of the COVID-19 pandemic, new generation vaccines are demanded. Among the current COVID-19 vaccines, a vaccine that can mimic the WT life cycle and be administered through intranasal can be favorably immunogenic and reduce viral shedding. Live-attenuated vaccine candidates are a straightforward example of this, which by their intranasal administration and mimicry of the WT SARS-CoV-2 life cycle can reduce viral shedding and restrict viral replication. As a result, a COVID-19 pandemic will be controlled. KaraVac, as a LAV candidate, may be a promising and feasible candidate vaccine to protect against the SARS-CoV-2 infection. We hope that the importance of using intranasal vaccines to combat the COVID-19 pandemic and other viral diseases will be much more significant soon.

Consent for publication

All authors agree to publish the article.

CRediT authorship contribution statement

Mohsen Abdoli: Methodology, Visualization, Investigation. **Maryam Shafaati:** Visualization, Investigation, Writing – original draft, Formal analysis, Writing – review & editing. **Ladan Kazem Ghamsari:** Methodology. **Asghar Abdoli:** Visualization, Investigation, Supervision, Writing – original draft, Formal analysis, Writing – review & editing.

Declaration of Competing Interest

The authors declare that there are no conflicts of interest.

References

Abdoli, A., Aalizadeh, R., Aminianfar, H., Kianmehr, Z., Teimoori, A., Azimi, E., Emamipour, N., Eghtedardoost, M., Siavashi, V., Jamshidi, H., 2021. Safety and potency of BIV1-CovIran inactivated vaccine candidate for SARS-CoV-2: a preclinical study. Rev. Med. Virol. e2305. https://doi.org/10.1002/rmv.2305.

Abdoli, A., Soleimanjahi, H., Kheiri, M.T., Jamali, A., Jamaati, A., 2013. Determining influenza virus shedding at different time points in Madin-Darby canine kidney cell line. Cell J. 15 (2), 130. Yakhteh.

Alu, A., Chen, L., Lei, H., Wei, Y., Tian, X., Wei, X., 2022. Intranasal COVID-19 vaccines: from bench to bed. EBioMedicine 76, 103841.

Assessment, R. R. SARS-CoV-2-increased circulation of variants of concern and vaccine rollout in the EU/EEA, 14th update.

Behloul, N., Baha, S., Shi, R., Meng, J., 2020. Role of the GTNGTKR motif in the N-terminal receptor-binding domain of the SARS-CoV-2 spike protein. Virus Res. 286, 198058.

Chan, J.F.W., Zhang, A.J., Yuan, S., Poon, V.K.M., Chan, C.C.S., Lee, A.C.Y., Chan, W.M., Fan, Z., Tsoi, H.W., Wen, L., 2020. Simulation of the clinical and pathological manifestations of coronavirus disease 2019 (COVID-19) in a golden Syrian hamster model: implications for disease pathogenesis and transmissibility. Clin. Infect. Dis. 71 (9), 2428–2446.

Chan, R.W., Liu, S., Cheung, J.Y., Tsun, J.G., Chan, K.C., Chan, K.Y., Fung, G.P., Li, A.M., Lam, H.S., 2021. The mucosal and serological immune responses to the novel coronavirus (SARS-CoV-2) vaccines. Front. Immunol. 4169.

Chan, Y.A., Zhan, S.H., 2020. Single source of pangolin CoVs with a near identical spike RBD to SARS-CoV-2. bioRxiv. doi:10.1101/2020.07.07.184374.

Chan, Y.A., Zhan, S.H., 2021. The emergence of the spike furin cleavage site in SARS-CoV-2. Mol. Biol. Evol. 39 (1), msab327. https://doi.org/10.1093/molbev/msab327.

Chen, J.M., 2021. Should the world collaborate imminently to develop neglected live-attenuated vaccines for COVID-19? J. Med. Virol. 94 (1), 82–87.

Clements, J.D., Freytag, L.C., 2016. Parenteral vaccination can be an effective means of inducing protective mucosal responses. Clin. Vaccine Immunol. 23 (6), 438–441.

Coelingh, K., Olajide, I.R., MacDonald, P., Yogev, R., 2015. Efficacy and effectiveness of live attenuated influenza vaccine in school-age children. Expert Rev. Vaccines 14 (10), 1331–1346.

Davidson, A.D., Williamson, M.K., Lewis, S., Shoemark, D., Carroll, M.W., Heesom, K.J., Matthews, D.A., 2020. Characterisation of the transcriptome and proteome of SARS-CoV-2 reveals a cell passage induced in-frame deletion of the furin-like cleavage site from the spike glycoprotein. Genome Med. 12 (1), 1–15. https://doi.org/10.1186/s13073-020-00763-0.

Guerrieri, M., Francavilla, B., Fiorelli, D., Nuccetelli, M., Passali, F.M., Coppeta, L., Somma, G., Bernardini, S., Magrini, A., Di Girolamo, S., 2021. Nasal and salivary mucosal humoral immune response elicited by mRNA BNT162b2 COVID-19 vaccine compared to SARS-CoV-2 natural infection. Vaccines 9 (12), 1499.

Hikmet, F., Méar, L., Edvinsson, Å., Micke, P., Uhlén, M., Lindskog, C., 2020. The protein expression profile of ACE2 in human tissues. Mol. Syst. Biol. 16 (7), e9610. https://doi.org/10.15252/msb.20209610.

Hoft, D.F., Lottenbach, K.R., Blazevic, A., Turan, A., Blevins, T.P., Pacatte, T.P., Yu, Y., Mitchell, M.C., Hoft, S.G., Belshe, R.B., 2017. Comparisons of the humoral and cellular immune responses induced by live attenuated influenza vaccine and inactivated influenza vaccine in adults. Clin. Vaccine Immunol. 24 (1), e00414–e00416.

Isabel, S., Graña-Miraglia, L., Gutierrez, J.M., Bundalovic-Torma, C., Groves, H.E., Isabel, M.R., Eshaghi, A., Patel, S.N., Gubbay, J.B., Poutanen, T., 2020. Evolutionary and structural analyses of SARS-CoV-2 D614G spike protein mutation now documented worldwide. Sci. Rep. 10 (1), 1–9.

Jin, X., Xu, K., Jiang, P., Lian, J., Hao, S., Yao, H., Yang, Y., 2020. Virus strain from a mild COVID-19 patient in Hangzhou represents a new trend in SARS-CoV-2 evolution potentially related to Furin cleavage site. Emerg. Microbes Infect. 9 (1), 1474–1488. https://doi.org/10.1080/22221751.2020.1781551.

Johnson, B.A., Xie, X., Bailey, A.L., Kalveram, B., Lokugamage, K.G., Muruato, A., Zou, J., Zhang, X., Juelich, T., Smith, J.K., 2021. Loss of furin cleavage site attenuates SARS-CoV-2 pathogenesis. Nature 591 (7849), 293–299.

Ketas, T.J., Chaturbhuj, D., Portillo, V.M.C., Francomano, E., Golden, E., Chandrasekhar, S., Debnath, G., Diaz-Tapia, R., Yasmeen, A., Kramer, K.D., 2021. Antibody responses to SARS-CoV-2 mRNA vaccines are detectable in saliva. Pathog. Immun. 6 (1), 116.

Kyriakidis, N.C., López-Cortés, A., González, E.V., Grimaldos, A.B., Prado, E.O., 2021. SARS-CoV-2 vaccines strategies: a comprehensive review of phase 3 candidates. NPJ Vaccines 6 (1), 1–17.

Lau, S.Y., Wang, P., Mok, B.W.Y., Zhang, A.J., Chu, H., Lee, A.C.Y., Deng, S., Chen, P., Chan, K.H., Song, W., 2020. Attenuated SARS-CoV-2 variants with deletions at the S1/S2 junction. Emerg. Microbes Infect. 9 (1), 837–842.

Lavelle, E.C., Ward, R.W., 2022. Mucosal vaccines—fortifying the frontiers. Nat. Rev. Immunol. 22 (4), 236–250.

Ma, Q., Li, R., Pan, W., Huang, W., Liu, B., Xie, Y., Wang, Z., Li, C., Jiang, H., Huang, J., 2020. Phillyrin (KD-1) exerts anti-viral and anti-inflammatory activities against novel coronavirus (SARS-CoV-2) and human coronavirus 229E (HCoV-229E) by suppressing the nuclear factor kappa B (NF-κB) signaling pathway. Phytomedicine 78, 153296.

Maassab, H., 1999. Principle of cold-adaptation in the derivation of live attenuated respiratory virus vaccines. Biotechnological Applications of Cold-Adapted Organisms. Springer, pp. 87–100.

Mengist, H.M., Kombe, A.J.K., Mekonnen, D., Abebaw, A., Getachew, M., Jin, T., 2021. Mutations of SARS-CoV-2 spike protein: implications on immune evasion and vaccine-induced immunity. Semin. Immunol. 55, 101533. Vol.

Miller, J., Ulrich, R., 2001. On the analysis of psychometric functions: the Spearman-Kärber method. Percept. Psychophys. 63 (8), 1399–1420.

Nunnally, B.K., Turula, V.E., Sitrin, 2015. Vaccine Analysis: Strategies, Principles, and Control. Springer. https://link.springer.com/book/10.1007/978-3-662-45024-6?noAccess=true.

Oh, J.E., Song, E., Moriyama, M., Wong, P., Zhang, S., Jiang, R., Strohmeier, S., Kleinstein, S.H., Krammer, F., Iwasaki, A., 2021. Intranasal priming induces local lung-resident B cell populations that secrete protective mucosal antiviral IgA. Sci. Immunol. 6 (66), eabj5129.

Okamura, S., Ebina, H., 2021. Could live attenuated vaccines better control COVID-19? Vaccine 39 (39), 5719–5726. https://doi.org/10.1016/j.vaccine.2021.08.018.

Pradhan, P., Pandey, A.K., Mishra, A., Gupta, P., Tripathi, P.K., Menon, M.B., Kundu, B., 2020. Uncanny similarity of unique inserts in the 2019-nCoV spike protein to HIV-1 gp120 and Gag. BioRxiv. doi:10.1101/2020.01.30.927871.

Sasaki, M., Toba, S., Itakura, Y., Chambaro, H.M., Kishimoto, M., Tabata, K., Sawa, H., 2021. SARS-CoV-2 bearing a mutation at the S1/S2 cleavage site exhibits attenuated virulence and confers protective immunity. Mbio 12 (4), e01415–21. https://doi.org/10.1128/mBio.01415-21.

Seo, S.H., Jang, Y., 2020. Cold-adapted live attenuated SARS-Cov-2 vaccine completely protects human ACE2 transgenic mice from SARS-Cov-2 infection. Vaccines 8 (4), 584.

van Tol, S., Mögling, R., Li, W., Godeke, G.J., Swart, A., Bergmans, B., Brandenburg, A., Kremer, K., Murk, J.L., van Beek, J., 2020. Accurate serology for SARS-CoV-2 and common human coronaviruses using a multiplex approach. Emerg. Microbes Infect. 9 (1), 1965–1973.

Wang, P., Lau, S.Y., Deng, S., Chen, P., Mok, B.W.Y., Zhang, A.J., Lee, A.C.Y., Chan, K.H., Tam, R.C.Y., Xu, H., 2021a. Characterization of an attenuated SARS-CoV-2 variant with a deletion at the S1/S2 junction of the spike protein. Nat. Commun. 12 (1), 1–10.

Wang, Y., Yang, C., Song, Y., Coleman, J.R., Stawowczyk, M., Tafrova, J., Tasker, S., Boltz, D., Baker, R., Garcia, L., 2021b. Scalable live-attenuated SARS-CoV-2 vaccine candidate demonstrates preclinical safety and efficacy. In: Proceedings of the National Academy of Sciences, 118.

World Health Organization, 2020. Laboratory Biosafety Guidance Related to Coronavirus Disease 2019 (COVID-19): Interim Guidance. W.H.O., 12 February 2020

Wu, S., Huang, J., Zhang, Z., Wu, J., Zhang, J., Hu, H., Zhu, T., Zhang, J., Luo, L., Fan, P., 2021. Safety, tolerability, and immunogenicity of an aerosolised adenovirus type-5 vector-based COVID-19 vaccine (Ad5-nCoV) in adults: preliminary report of an open-label and randomised phase 1 clinical trial. Lancet Infect. Dis. 21 (12), 1654–1664.

Zhang, A. J., Chen, H., 2020. Pathogenicity, immunogenicity, and protective ability of an attenuated SARS-CoV-2 variant with a deletion at the S1/S2 junction of the spike protein. BioRxiv. doi:10.1101/2020.08.24.264192.

Yaqinuddin, A., Kazkaz, H., MishariAlSaud, M., Khaled, A., Kashir, J., 2021. Advantageous non-specific effects of live-attenuated vaccines in COVID-19 treatment. Afr. J. Respir. Med. 16.

Xi, J., Lei, L.R., Zouzas, W., April Si, X., 2021. Nasally inhaled therapeutics and vaccination for COVID-19: developments and challenges. MedComm. 2(4), 569-586. doi:10.1002/mco2.101.